

SEISMIC PERFORMANCE OF DUCTILE AND NON-DUCTILE DETAILED BEAM-COLUMN SUB-ASSEMBLAGES

A.Kanchana Devi¹, Saptarshi Sasmal², K.Ramanjaneyulu³

¹Academy of Scientific and Innovative Research, CSIR-Structural Engineering Research Centre, Chennai, India,

²Academy of Scientific and Innovative Research, CSIR-Structural Engineering Research Centre, Chennai, India,

³Academy of Scientific and Innovative Research, CSIR-Structural Engineering Research Centre, Chennai, India,

kanchana@serc.res.in, saptarshi@serc.res.in, rams@serc.res.in

Abstract

Reinforced concrete(RC) framed joints are the crucial components as they are subjected to huge shear demand nearly 4-6 times larger than the adjoining members under earthquake. Hence, seismic performance of beam-column joints is evaluated for two scenarios viz., i) beam column joints designed for seismic force but not provided with ductility detailing (non- ductile specimen) ii) designed for seismic force and provided with ductility detailing according to code of practice. An exterior joint of a typical three storied three bay RC Framed building is considered for the study. The frame is designed considering all the combinations of loads specified in code of practice. The performance of the beam-column sub-assembly is evaluated in terms of performance parameters, namely, load- displacement hysteresis, energy dissipation, strength and stiffness degradation. Even though the non-ductile specimen has slightly higher beam reinforcement than the ductile specimen, the ductile specimen carried higher load than the non-ductile specimen in the view of detailing in joint region. This may be due to the confinement effect provided by the stirrups in the joint region in the view of closer spacing as per ductile detailing. The maximum load carried by ductile detailed specimen in the positive and negative cycles is 39% and 9% higher than that of non-ductile specimen. This signifies the importance of ductility detailing.

Keywords: Beam column sub-assembly, seismic performance, ductility detailing, Energy dissipation, strength degradation

INTRODUCTION

In RC framed structures, beam-column joints are crucial members as i) they dissipate the seismic energy imparted to the structure ii) hinder the force flow mechanism iii) if they fail it is difficult to repair a joint region and iv) joint deformation will increase the storey drift. According to the capacity design philosophy of strong column - weak beam, the flexural failure of beam is preferable as it is ductile mode of failure and dissipates more energy compared to other failure modes. In order to achieve these, different codes of practices, namely, Euro, ACI, NZ codes prescribe appropriate detailing practices so that the brittle failure could be avoided. The concept of ductility detailing was recognised globally during late 70s and were incorporated in the codes of practices during 80s. Hence, investigations on the seismic performance of beam-column joint which are detailed differently give insight into its behaviour and thereby enabling the suitable formulations to improve its seismic performance.

Remarkable change in the design philosophies of RC framed structures for seismic resistance was made after the pioneering works of Megget and Park (1971), Park and Paulay (1973), Blakeley et al (1975), Paulay, Park and Priestley (1978), Park and YeohSikkeong(1979), Ehsani and Wight (1985). Murty et al (2003) conducted experimental investigation on the exterior RC joint with four details of longitudinal beam bar anchorage and three details of

transverse joint reinforcement. The longitudinal bars are provided as U bars, standard ACI 90 hook, full anchorage of beam top and bottom bars and full anchorage of beam top bars and straight beam bottom bars. The transverse reinforcements are varied as closed ties, hair clips and no ties in the joint region. It was reported that the seismic performance of non-seismically designed structures could be improved by proper anchorage of longitudinal reinforcement and providing lateral reinforcement. It was also observed that ACI standard hook with hair clip type transverse reinforcement is preferable as it was easy to construct and effective when compared to the other schemes considered. Ramanjaneyulu et al. (2013) evaluated the seismic performance of exterior beam-column sub-assemblages by considering different evolution stages of Eurocode (EC) and Indian Standard (IS). It is found that the gravity load designed (GLD) structure is vulnerable to even medium intensity earthquake. Masi et al (2013) analysed the experimental results of gravity load designed and seismic load designed specimens tested in the University of Basilicata in Potenza, Italy. The numerical simulations are also carried out to understand the behaviour and to evaluate the stress distribution in the joint panel zone as function of axial load and to quantify the beam rebars deformation. From the study, two failure modes were observed i) mixed mode involving beam and joint damage ii) flexural failure involving beam only. It was also observed that mixed mode of failure reduces the deformation capacity.

In the present study, seismic performance of beam-column joints is evaluated for two scenarios viz., i) beam-column joints designed for seismic force but not provided with ductility detailing (non-ductile specimen) ii) designed for seismic force and provided with ductility detailing according to Indian code of practice. The performance of the beam-column sub-assembly is evaluated in terms of performance parameters, namely, load-displacement hysteresis, energy dissipation, strength and stiffness degradation.

DETAILS OF SPECIMEN

A typical three storied RC Framed building with 6m span and 3.5m floor height each is analysed for dead load, live load and seismic loads. The seismic loads are arrived according to IS1893 based on equivalent seismic load method. For the computation of base shears due to seismic load, the horizontal seismic acceleration coefficient is estimated with the response reduction factor of 3 and 5 respectively for non-ductile (SP2) and ductile specimens (SP3). Beams and columns are designed for worst combination of forces as per IS standards as 1.5DL+1.5LL, 1.5DL+1.5EL, 1.5DL-1.5EL, 1.2DL+1.2LL+1.2EL and 1.2DL+1.2LL-1.2EL. The cross section dimensions of 300mmx400mm and 300mmx300mm are adopted for beam and column respectively for both ductile and non-ductile specimens. The non-ductile specimen is detailed according to SP34 whereas ductile specimen is detailed according to the IS 13920. The specimens are instrumented extensively by affixing strain gages at critical locations identified on the reinforcement bars. Strain gages are affixed on the main reinforcement bars of the beam near the junction upto the distance 'd', i.e. the depth of the beam and on the column main bars, column ties and beam stirrups. The concrete of mix proportions 1:1.695:3.013 with water cement ratio of 0.5 is used. The specimens are cast and are cured for 28 days using wet curing. The reinforcement details are given in the Figures 1 and 2 for SP2 and SP3 specimen respectively. The concrete cubes and cylinders which were cast along with the specimen were tested and the average compressive strength and split tensile strength of concrete are presented in Table 1.

Experimental Investigations

The test specimens are also instrumented with LVDTs (linear variable displacement transducers), which are mounted on the joint surface as well as attached to the beam and the column segments to measure deflections along the length of beam and column segments and to calculate the rotation of the joint. The test setup is arranged on the test floor so that the beam-column joint is positioned horizontally parallel to the floor and the cyclic load is applied in the plane of the test floor. The schematic diagram of test set-up and positioning of test specimen is shown in the Fig.3a. An axial load of 300kN is applied to the column by hydraulic jack at one end of the column against the reaction block at the other end. The level of axial load in column was arrived by analysis of the global system of the

three storey four bay building. The lateral load was applied on the beam tip in displacement control mode using 25t actuator, according to the load history shown in Fig. 3b. Reverse cyclic load is applied in terms of drift ratio (%) of the component where the drift is calculated as per equation (1).

$$\text{Drift ratio (\%)} = (\Delta l / l_b) \times 100 \quad (1)$$

Where, Δl and l_b are the applied displacement at the beam tip and the length of the beam from column face to the application point of the displacement respectively. Three complete cycles are applied at each drift ratio.

Progressive Cracking

For specimen SP2, the first flexural cracks are developed at the face of the joint in beam top and bottom at the drift ratio of 0.367%. The flexural cracks spread throughout the twice the depth of the beam till the drift ratio of 1.47%. At the drift ratio of -0.735%, the diagonal shear cracks appeared along diagonal connecting beam bottom and column outer face. At drift ratio of 1.47%, the shear cracks appeared along the diagonal connecting beam top and column outer face. At the drift ratio of 2.2%, flexural cracks appeared at the outer face of column. As the joint is provided with horizontal ties and the beam bottom as well as top bars are anchored, the diagonal cracks widened in both directions with the further increment of drift ratio. The diagonal strut mechanism could be mobilized along both diagonals of the joint which is evident from Fig.4a. After the yielding of beam reinforcement, the damage is shifted to joint region and resulted in the severe joint damage. During the final stage of loading, at $\pm 5.88\%$ drift ratio, upheaving of concrete in the joint region and opening of joint is observed as shown in Fig. 4b.

In specimen SP3, at drift ratio of 0.367%, first flexural cracks are appeared at the joint face at the beam bottom and but the first flexural crack on the beam top is appeared at the drift ratio of 0.735%. The flexural cracks spread throughout the length of beam with increment of drift. The first diagonal shear cracks are formed in the joint at the drift ratio of 1.47%. As the joint is provided with confinement in the form closely spaced ties and the presence of intermediate column bars enables mobilisation of shear resistance through compression strut, vertical and horizontal mechanism which is evident from the crack pattern observed. At the final stage of loading (at $\pm 7.05\%$ drift ratio) column cover concrete at the outer face of column spalled-off and upheaving of joint concrete is also observed as shown in Fig.5.

Results and Discussions

Load Displacement hysteresis

The load versus displacement hystereses obtained from the experiments are presented in Figs 6 and 7. The maximum load carried by the SP2 and SP3 specimens in the positive cycle (i.e., tension on Beam bottom) are 58kN and 94kN

respectively. The higher load carried by ductile specimen is due to provision of positive steel at the joint face equal to at least 50% of negative steel at that face from ductility detailing consideration. In the negative cycle, maximum load carried by the SP2 and SP3 specimens are 112kN and 123kN respectively. Even though the non-ductile specimen has slightly higher reinforcement than the ductile specimen, the ductile specimen carried higher load than the non-ductile specimen. This may be due to the confinement effect provided by the ties in the joint region. In the negative cycle, both specimens exhibited almost similar hysteric behavior. Whereas in the positive cycle remarkable improvement in the hysteric behaviour is observed. The maximum load carried by SP3 in the positive and negative cycles is 39% and 9% higher than SP2 respectively. Even though the total area of steel (ie including main steel of beam, column and stirrups) provided in the both specimens are almost same ductile specimen showed remarkable performance. This signifies the importance of providing ductility detailing. Though the seismic performance of SP3 is superior to SP2, weak beam-strong column mode of failure is not observed in the both specimens.

Load versus displacement envelopes obtained for both specimens are depicted in Figure 8. It could be observed that the ductile specimen carried much higher load for all the displacement levels in the positive cycle. In the negative cycle, both specimen carried almost same envelope load till 37.5mm displacement level (i.e., till the yielding of steel reinforcement) but ductile specimen carried much higher load beyond 37.5mm displacement cycles. The ductile specimen sustained maximum displacement of 120mm whereas the non-ductile specimen could sustain maximum displacement of 100mm at beam tip.

Energy dissipation

The energy dissipation is the crucial performance parameter as the most of the seismic design principles rely on the inelastic deformation of the structure to withstand severe earthquakes. It is highly essential to ensure the required energy dissipation to prevent collapse of structures during severe earthquake. The cumulative energy dissipation capacity of specimen is shown in Fig 9. The cumulative energy dissipated by specimen SP2 and SP3 are almost same during the initial cycles up to the drift ratio of 2.2% (up to yielding of steel reinforcement). After the drift level of 2.2%, the cumulative energy dissipation of ductile specimen is much larger than that of SP2. The cumulative energy dissipation of SP3 is 2.5 times larger than that of SP2. Even though the maximum load carried by both specimens are nearly same, the energy dissipated by SP3 is enormous when compared to that of SP2. Thus energy dissipation depends on the ductility rather than on the strength of the specimen.

Stiffness degradation

The stiffness degradation of the specimens is shown in Fig 10. Before failure all the specimens have undergone severe damage in the form of flexural cracks, shear cracks and up

heaving of concrete at the joint due to excessive shear deformation. This resulted in huge stiffness degradation of above 90% in both the specimens. Stiffness degradation of specimen SP3 is lower than SP2 in both positive and negative cycles for all the drift ratios. At drift ratio of 2.2%, stiffness degradation in first cycle of SP3 is 8% in positive cycle and in the corresponding negative cycle it is 11%, lower than SP2. It is observed that stiffness degradation in the positive cycles is more than the stiffness degradation in the negative cycle for both SP2 and SP3. At drift ratio of 2.2%, stiffness degradation of first positive cycle is 14% and 12% lower than corresponding negative cycle in SP3 and SP2 respectively.

Strength degradation

The strength degradation in second and third cycles with respect the first cycle at each drift ratio is shown in Fig 11. It is observed that the strength degradation in the positive cycles is larger than the negative cycle for SP2 whereas SP3 has undergone equal degradation in both positive and negative cycles. Even though SP2 is designed for higher seismic forces than SP3 the strength degradation of SP2 is much larger than SP3 in both positive and negative cycles. Strength degradation of SP3 is less than 10% till the drift ratio of 3.67% in both positive and negative cycles. The maximum strength degradation of SP3 and SP2 in positive cycles is 17% and 28% respectively and in negative cycles are 19% and 23% respectively. Specimen SP2 has larger beam top reinforcement than SP3 but still the strength degradation and maximum load carried by SP2 is larger than SP3. The confinement provided by the ties/stirrups improves the load carrying capacity and reduces further damage.

After the yielding of beam reinforcement, specimen SP2 showed global strength degradation i.e. degradation in strength with drift increment behavior in both positive and negative cycles. In specimen SP3, the negative cycles showed a global strength degrading behavior whereas in the positive cycles the load sustained from a drift ratio of 2.2% to 3.6% beyond which global strength degradation behavior was observed.

CONCLUSIONS

Seismic performance of ductile and non-ductile exterior beam column sub-assembly specimens are evaluated by conducting reverse cyclic load test. The performance of the beam-column sub-assembly is evaluated in terms of performance parameters, namely, load- displacement hysteresis, energy dissipation, strength and stiffness degradation. The maximum load carried by ductile detailed specimen in the positive and negative cycles is 39% and 9% higher that of non-ductile specimen. The cumulative energy dissipation of SP3 is 2.5 times larger than SP2. Even though the maximum loads carried by both specimens are nearly same, the energy dissipated by SP3 is enormous when compared to SP2. Stiffness degradation of specimen SP3 is lower than that of SP2 in both positive and negative cycles for all the drift ratios. The maximum strength degradation of SP3 and SP2 in positive cycles is 17% and 28% respectively

and in negative cycles are 19% and 23% respectively. Though the seismic performance of SP3 is superior to SP2 weak beam-strong column mode of failure is not observed in both the specimens. Thus, the present study enlightens on the behavior of specimen that are designed with prevailing code and also be useful to improve the empirical and too general provisions of code.

Acknowledgement

This paper is being published with the kind permission of the Director, CSIR-SERC, Chennai.

REFERENCES

[1] Blakeley, R.W.G., Megget, L.M. and Priestley, M.J.N., "Seismic Performance of Two Full Size Reinforced Concrete Beam-Column Joint Units", Bulletin of the New Zealand National Society for Earthquake Engineering, Vol. 8, No. 1, March 1975, pp. 38-69

[2] Ehsani, M. R. and Wight J.K., "Exterior reinforced concrete beam to column connections subjected to Earthquake -type loading", ACI Journal, 1985, pp 492-499.

[3] Masi A., Santarsiero G., Lignola G. P., and Verderame G.M., "Study of the seismic behaviour of external RC beam-column joints through experimental tests and numerical simulations", Engineering structure, Vol. 52, available online from March 2013, pp 207-219.

[4] Megget, L.M. and Park, R., "Reinforced Concrete Exterior Beam-Column Joints Under Seismic Loading",

New Zealand Engineering, Vol. 26, No. 11, 1971, pp. 341-353.

[5] Murty C.V.R., Rai D.C., Bajpai K.K., and Jain S.K., "Effectiveness of reinforcement details in exterior reinforced concrete beam-column joints for earthquake resistance", ACI Structural Journal, V. 100, No. 2, March-April 2003, pp 149-156.

[6] Park, R. and Paulay, T., "Behaviour of Reinforced Concrete External BeamColumn Joints Under Cyclic Loading", Proceedings, Fifth World Conference on Earthquake Engineering Paper 88, Vol. 1, Session 2D, Rome, June 1973, pp. 772-781

[7] Park, R. and YeohSikKeong, "Tests on Structural Concrete Beam-Column Joints with Intermediate Column Bars", Bulletin of the New Zealand National Society for Earthquake Engineering, Vol. 12, No. 3, September 1979, pp. 2361-2376

[8] Paulay, T., Park, R. and Priestley, M.J.N., "Reinforced Concrete BeamColumn Joints Under Seismic Actions", Journal of the American Concrete Institute, Proceedings, Vol. 75, No. 11, November 1978, pp. 585-593

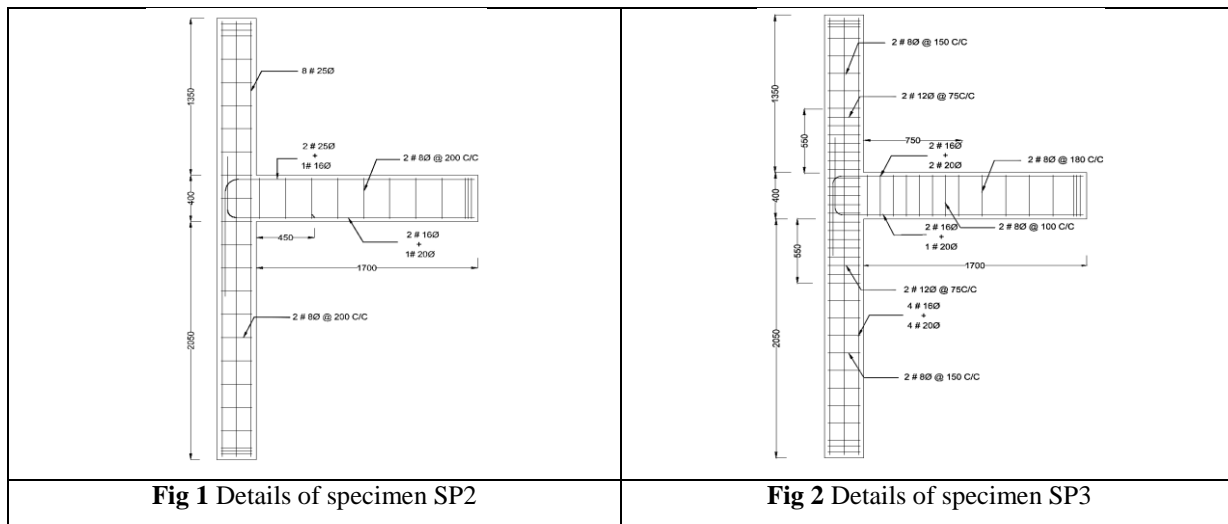
[9] Paulay T, Priestley MJN., "Seismic design of reinforced concrete and masonry buildings", New York: John Wiley Publications; 1992

[10] Ramanjaneyulu, K., Novák, B., Sasmal, S., Roehm, C., Lakshmanan, N., and Nagesh R. Iyer. (2013), "Seismic performance evaluation of exterior beam column sub-assemblages designed according to different codal recommendations", Structure and Infrastructure Engineering, V.9(8), 817-833.

Table 1 Strength parameters of concrete

Specimen	Average cube compressive strength of concrete (N/mm ²)	Average cylinder compressive strength of concrete (N/mm ²)	Average split tensile strength of concrete (N/mm ²)
Non ductile	46.75	34.66	2.87
Ductile	55.41	34.72	2.75

Figures



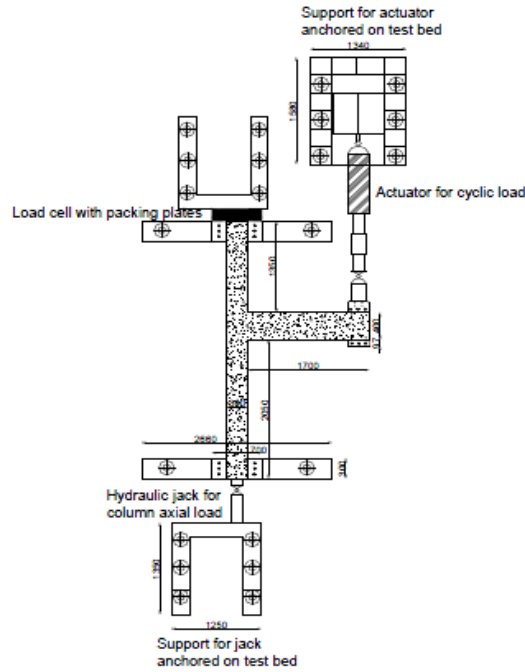


Fig 3a Set up for experimental investigation

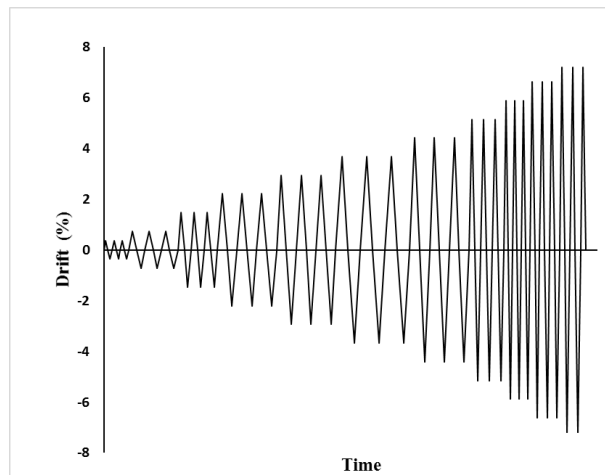


Fig 3b Reverse cyclic loading history

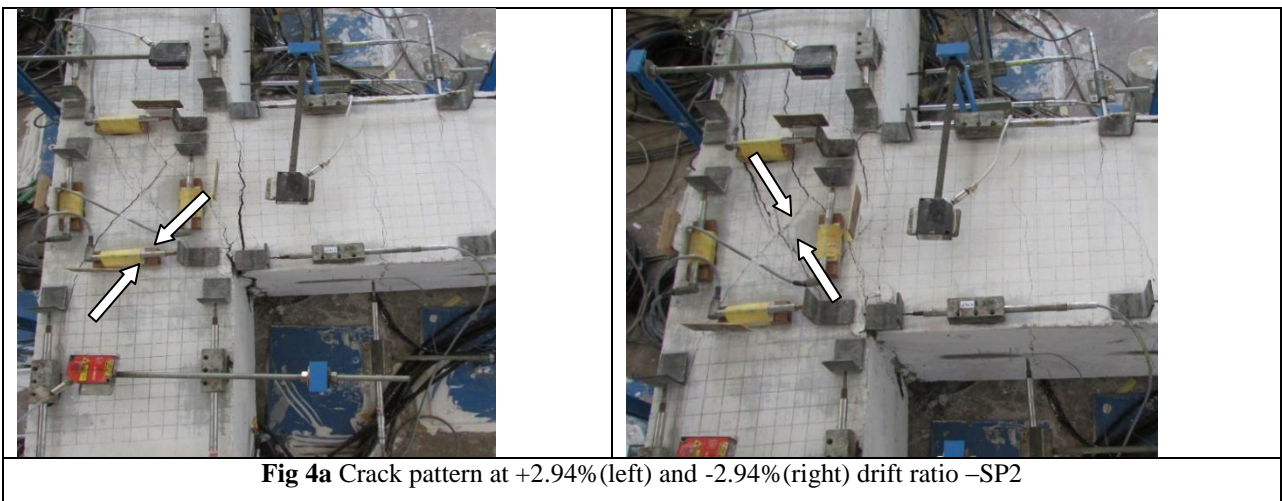


Fig 4a Crack pattern at +2.94% (left) and -2.94% (right) drift ratio –SP2



Fig 4b Crack pattern at +5.88%(left) and -5.88%(right) drift ratio –SP2



Fig 5 Crack pattern at +7.05%(left) and -7.05%(right) drift ratio –SP3

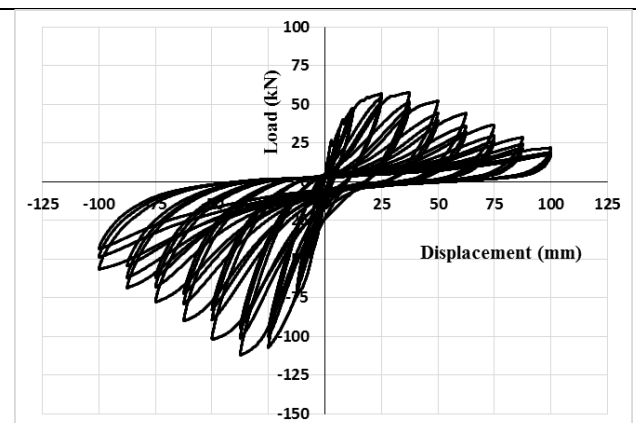


Fig. 6 Load Displacement hysteresis of SP2

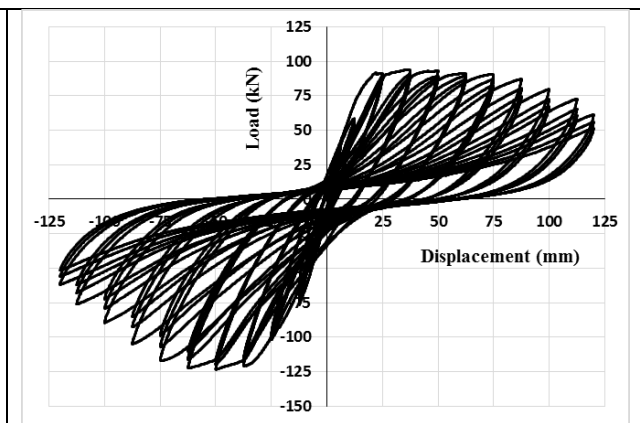


Fig. 7 Load Displacement hysteresis of SP3

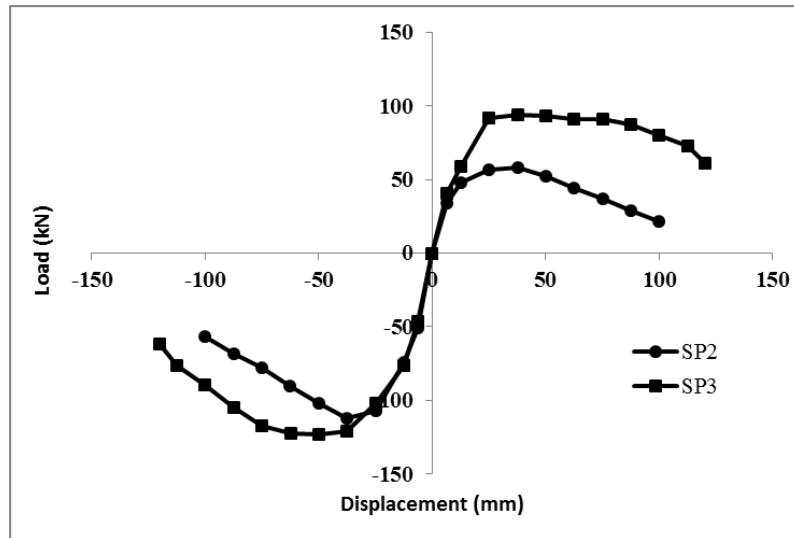


Fig. 8 Load Envelope of specimens SP2 and SP3

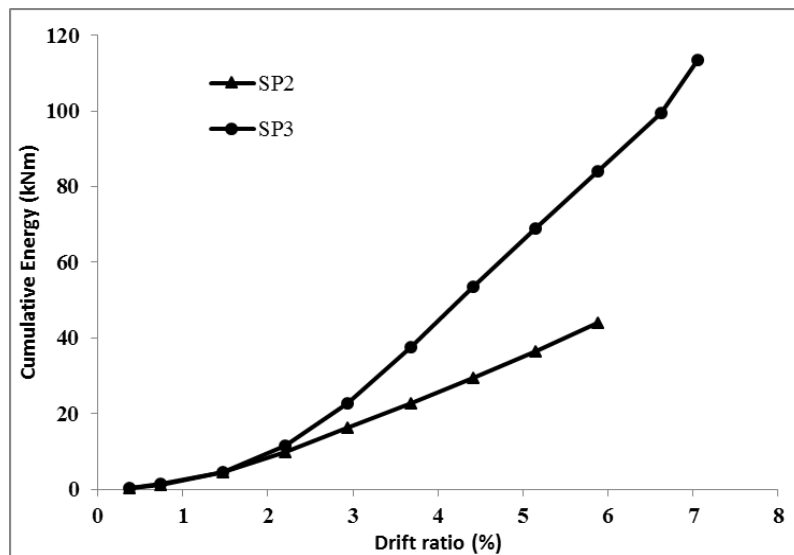


Fig. 9 Cumulative energy dissipation

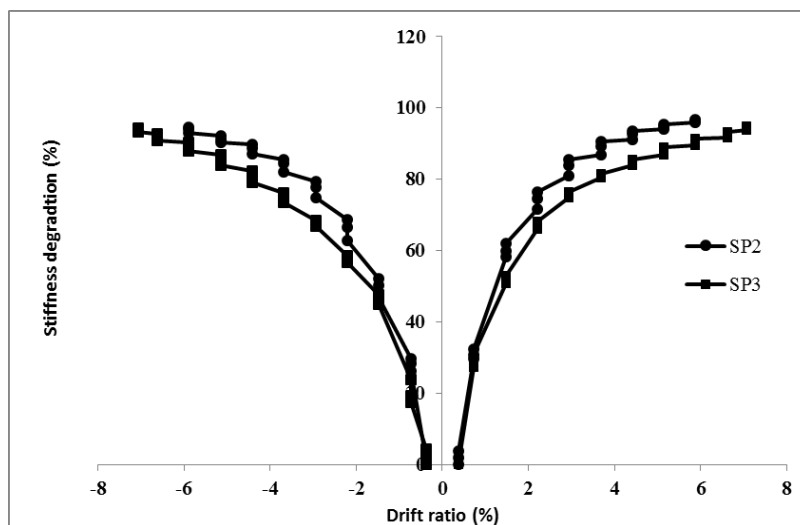


Figure 10 Stiffness Degradation of specimens

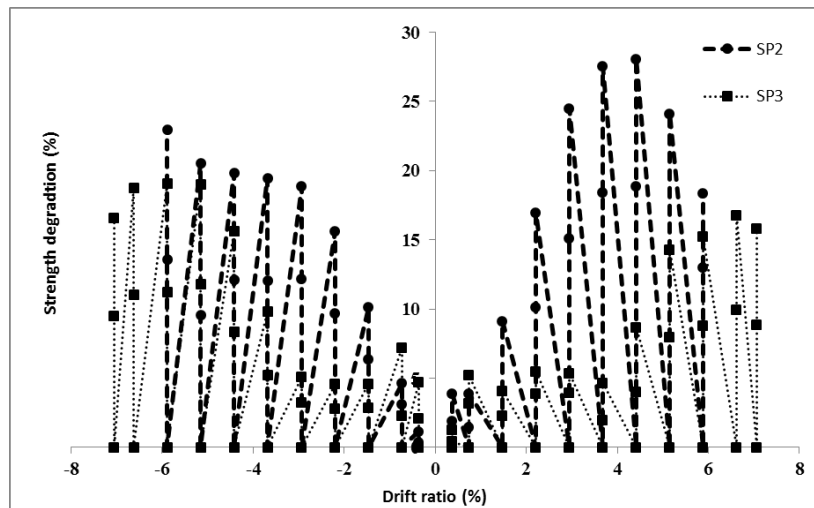


Figure 11 Strength Degradation of specimens